Vietnam Journal of Earth Sciences, 45(2), 199-218, https://doi.org/10.15625/2615-9783/18303

Vietnam Journal of Earth Sciences
https://vjs.ac.vn/index.php/jse

Monitoring the storage volume of impounding reservoirs in inaccessible regions using multi-sensor satellite data: the case study of Tuyen Quang Reservoir (Vietnam)

Nguyen Thien Phuong Thao[1], Nguyen Duy Thai[1], Nguyen Thi Thu Ha[1,*], Pham Quang Vinh[2], Dinh Xuan Thanh[1]

[1]*Faculty of Geology, VNU University of Science, Hanoi, Vietnam*
[2]*Institute of Geography, VAST, Hanoi, Vietnam*

Received 15 August 2022; Received in revised form 26 December 2022; Accepted 24 April 2023

ABSTRACT

Water stored by reservoirs is critical for irrigation, electricity generation, drinking water supply, recreation, fisheries, and flood control. Therefore, the reservoir's water storage volume (SW) must be measured and monitored frequently for better watershed management. Since SW data is often not publicly available, finding a method to quantify SW objectively and accurately but to facilitate local water management is necessary. This study proposes a method for monitoring water surface area and storage volume using multi-sensor satellite remote sensing data through the Tuyen Quang Reservoir case study in Northern Vietnam. Accordingly, the water surface area was first delineated from multi-temporal optical satellite images, such as Landsat series and Sentinel-2 images, using the Modified Normalized Difference Water Index and resampled into 30-m pixel resolution data. Using the Shuttle Radar Topography Mission Digital Elevation Model data, the water depth at each pixel was then calculated by the difference between its elevation and the reservoir shoreline's mean elevation. The results showed that the reservoir's water surface area increased rapidly during 2003-2007 (from 579 ha to 5,516 ha), fluctuated insignificantly in 2008-2020, and reached 7,196 ha in 2021. Consequently, SW was raised from 11.8 million m^3 in 2003 to 1.68 billion m^3 in 2021. Our estimations agree with the depth and SW of Tuyen Quang Reservoir published in 2019. Our proposed method could be an effective water resource management tool in developing countries where the number of impounding reservoirs increases dramatically yearly without the financial afford to build gauging stations.

Keywords: Reservoir capacity, Bathymetry, SRTM DEM, Sentinel-2, Landsat imageries, MNDWI.

1. Introduction

Many thousands of reservoirs have been constructed worldwide during the last decades to provide water for irrigation, electricity generation, fisheries, and tourism (World Commission on Dams, 2000; Yoshikawa et al., 2013). For instance, there were 3,700 reservoirs under construction in 2014, most of which were in developing countries in South America, Southeast Asia, and Africa (Zarfl et al., 2015). However, the massive development of reservoirs has led to an imbalance of water resources in rivers and even a loss of water sources in many reservoirs (Kellner, 2021). Additionally, with the projected population increase, demands for water for food

*Corresponding author, Email: hantt_kdc@vnu.edu.vn

production and electricity also increase substantially, requiring intensive water withdrawal levels, which could deplete water supply sources or even cause them to run dry in many countries. Furthermore, the determination of reservoir properties, including water surface area (WA), water depth (WD), and water storage volume (SW), plays a crucial role in detecting many environmental changes such as sedimentation, ecosystem functioning, lifetimes, and the derivation of erosion and sedimentation rates of catchments (Dost & Mannaerts, 2008). Therefore, knowledge of temporal changes in the SW of a reservoir is critical for managing water resources within the basin and interpreting the possible impacts of climate change.

SW is the net result of river inflows, evaporation, and dam water releases. Consequently, SW varies seasonally due to the change of precipitation and runoffs over the river's catchment and is depleted depending on the local water demands for irrigation and electricity generation. Generally, SW is traditionally estimated based on the observed water level (WL) at the gauging station installed in the reservoir and the total area of the reservoir using morphometric data (Hayashi & Van der Kamp, 2000; Brooks & Hayashi, 2002; Gamble et al., 2007; Gleason et al., 2007). However, the observed WL at the gauging station only reflects the depth at the station's location. It is not the mean depth of the reservoir. Moreover, the total area of the reservoir is not the actual WL. Therefore, the traditional method for estimating the SW of a reservoir is often inaccurate and over-estimated, causing challenges for dam operation and water resource management.

In many cases, no gauging station is installed in the reservoir (the general condition of small and inaccessible reservoirs), so the determination of WA, WD, and SW is often challenged. WA, WL, and SW are sometimes determined from fine-resolution topographic maps based on detailed survey data (Hayashi & Van der Kamp, 2000). However, topographic maps are often not updated even for a decade, and WL fluctuations are almost absent in these maps, making it difficult to detect the changes in WA, WL, and SW. For this reason, the information about reservoirs' properties is often not publicly available or published at the general level without updates. Therefore, finding a method to quantify WA, WD, and SW objectively and accurately but simply to facilitate local water management is necessary.

Remote sensing is widely used in lake and reservoir management for identifying, measuring, and characterizing the properties of lakes and reservoirs (Verpoorter et al., 2014; Chipman et al., 2009; Alsdorf et al., 2007; Gao et al., 2012). WA of lakes and reservoirs has been successfully mapped using optical and microwave sensors in environments from the tropics to the poles (Verpoorter et al., 2014; Chipman et al., 2009; Melack et al., 1994; Morriss et al., 2003; Yang and Chen, 2017; Gao, 1996; McFeeters, 1996; Feyisa et al., 2014; Hereher, 2015). Many methods have been developed for WA delineations from satellite images, of which using spectral indices such as the Normalized Difference Water Index, NDWI (McFeeters, 1996), the Normalized Difference Lake Index, NDLI (Morriss et al., 2003; Hereher, 2015) or the Automated Water Extraction Index, AWEI; (Feyisa et al., 2014) is often preferred because of its rapid, simple and accurate procedure. The vertical dimension of water volume (WL and WD) can also be measured using the laser (Chipman et al., 2007; Wang et al., 2011; Zhang et al., 2011; Arsen et al., 2013) or radar altimetry (Swenson & Wahr, 2009; Birkett, 2000; Crétaux & Birkelt, 2006; Pham-Duc et al., 2019; 2022). In some cases,

lake depths are also estimated from optical images such as Landsat-8 and Sentinel-2 (Pope et al., 2016; Duan et al., 2022). Launching the Surface Water and Ocean Topography (SWOT) satellite mission in December 2022 also supports remote sensing-based monitoring of lakes and reservoirs (Solander et al., 2016; Biancamaria et al., 2016). The above analyses show a high possibility of satellite data monitoring reservoirs' properties. Indeed, monitoring large global reservoirs using free satellites has been carried out with many positive results (Gao et al., 2012; Crétaux et al., 2011; 2016; Avisse et al., 2017). For small reservoirs, high spatial resolution digital elevation model (DEM) data such as the Shuttle Radar Topography Mission Digital Elevation Model (SRTM DEM, ~30 m resolution) or TanDEM-X (12 m resolution) can be used to estimate and monitor the SW (Vanthof et al., 2019).

According to the Directorate of Water Resources, Vietnam has built 7,342 reservoirs with a total SW of 14.5 billion m^3, providing water for irrigation of 1.1 million cultivated hectares and 1.5 billion m^3 for daily life and industry. Most reservoirs are distributed in inaccessible areas and must be monitored SW frequently, particularly in the wet season (Directorate of Water Resources, 2022). Due to limited finances, numerous small reservoirs do not have gauging stations. For reservoirs, which have severely damaged dams, frequent monitoring of SW becomes even more urgent. Therefore, identifying a scientific and technological solution to help monitor SW in those reservoirs accurately, quickly, and costly are extremely necessary. Up to the present, several studies attempted to use remote sensing in monitoring reservoirs' properties across the country, for example, the use of Sentinel-1 data for delineating WA, SW, and elevations of Song Rac, Ngan Truoi and Ke Go Reservoirs (Hiep & Hung, 2019); the use of Landsat-8 and Sentinel-2 data for monitoring WL and SW of Sesan 4 in 2019 (Tung et al., 2020); or monitoring the change of WA of Nui Coc reservoirs using Sentinel-1A data acquired during 2016-2020 (Binh & Son, 2022). Although approached on different aspects, these studies have demonstrated the high potential of remote sensing for monitoring SW in our country. However, these studies have not clearly shown the SW calculation procedure, particularly the absence of the depth retrieval method. An improved procedure needs to be established for more convenient monitoring of SW.

This study presents a method for monitoring WA, WD, and SW of Tuyen Quang Reservoir in the 2003-2021 period using free multispectral satellite images and SRTM DEM data. Our objectives are: (1) to determine the dynamics of Tuyen Quang Reservoir's WA in space and time for the period of 2003-2021; (2) to calculate and map the depths of the reservoir using the combination of DEM data and detected WA; (3) to demonstrate the reliability of the time-series SW estimated from remote sensing data.

2. Materials and Methods

2.1. Study Area

Tuyen Quang Reservoir, formerly Na Hang Reservoir, is located on the Gam River in Na Hang District, Tuyen Quang Province, Vietnam. Additional to Gam River, Tuyen Quang Reservoir also receives water from the Nang River and the local dense stream system (Fig. 1). The reservoir is recognized as the third largest reservoir in the North of Vietnam, after Son La and Hoa Binh Reservoirs. The reservoir was constructed on December 22, 2002, and completed in 2008. The reservoir plays an essential role in flood control for Tuyen Quang Province. It contributes to regulating floods in the Red River Delta, creating water sources for hydropower and irrigation in the Red River Delta in the dry season. Tuyen Quang Reservoir's catchment is in a high

mountainous area (200-600 m) where most of the area is covered by primary forest and Devonian limestones of Mia Le, Ban Pap, Ngan Son formations. The region is dominated by a tropical monsoon climate, receiving an average annual rainfall of 1,260 to 2,410 mm from two distinct seasons: the wet season from April to October (82-91% of the average annual rainfall) and the dry season from November to March. The region has a dense hydrological network, approximately 0.9 km/km^2, with many rapids and waterfalls (Tuyen Quang Provincial People Committee, 2014). Only a few studies investigated the reservoir's features, mainly focused on socio-tourism development in the region (Bon et al., 2014; Dine, 2012). Up to date, only general information of the reservoir has been addressed officially in the Vietnamese Minister's Decision on promulgating the Inter-reservoir Operation Procedures for the Red River basin, i.e., the mean water level is 120 m; total capacity is 2.26 billion m^3; useful capacity is 1.7 billion m^3.

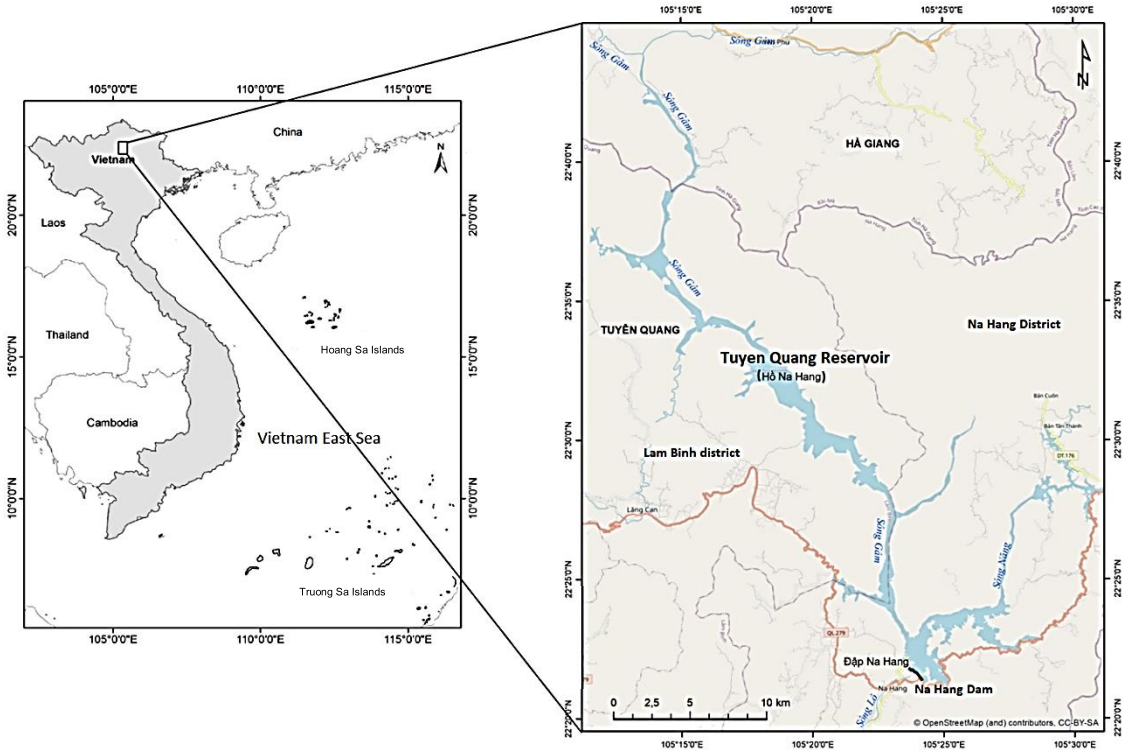

Figure 1. Location of the Tuyen Quang Reservoir in Vietnam (A) and relationships of the reservoir with Gam and Nang Rivers (B)

2.2. Used satellite data

The Landsat TM, ETM+, OLI, and Sentinel-2 MSI images were used to estimate the reservoir surface area from 2003 to 2021 (Table 1). This selection was made based on three principles: (1), both Landsat and Sentinel-2 data were used to detect the surface area of inland lakes in preceding studies (Li & Roy, 2017; Lu et al., 2013); (2), the 30 m resolution of Landsat data is suitable for representing the irregular shapes of many reservoirs (Pardo-Pascual, 2012; Yang et al., 2020); (3) data is free and processed into level 2, which provides the bottom of atmosphere reflectance data, before delivering to users via the data portals of United States Geological

Survey (https://earthexplorer.usgs.gov/) and The European Space Agency (https://scihub.copernicus.eu/). The entire Tuyen Quang Reservoir fits in a Landsat scene in the path/row of 127/44 of the TM and the ETM+ images and 127/45 of the OLI image. For Sentinel-2 MSI images, the reservoir is distributed in two consecutive scenes with the codes T48QWK and T48QWL of the data grid system (Table 1). To unify the spatial resolution of the data for a better comparison with Landsat-derived data conventionally and to fit the DEM data, the Sentinel-2 MSI data was resampled to 30 m resolution using the nearest neighbor algorithm in the SNAP 8.0.

Table 1. Information on satellite images used in this study

	Sensor	Path/row	Date of Acquisition (date/month/year)	Resolution (m)
Landsat	TM	127/44	23/12/2003	30
			09/10/2005	
			05/11/2009	
			08/11/2010	
Landsat	ETM+	127/44	05/11/2006	30
			08/11/2007	
			10/11/2008	
Landsat	OLI	127/45	18/12/2013	30
			07/10/2016	
			03/12/2019	
Sentinel	2B	T48QWK T48QWL	25/12/2017	10 & 20
			31/10/2018	
			2/06/2021	
			04/12/2021	
Sentinel	2A	T48QWK T48QWL	09/03/2020	10 & 20
			26/08/2020	
			14/11/2020	
			13/01/2021	
			10/09/2021	
			19/12/2021	

The DEM (Digital Elevation Model) data used in this study is the SRTM 1Arc-Second Global Version 3.0 (SRTM Plus, 30 m resolution), which includes topographic data from non-SRTM sources to fill the gaps ("voids") in earlier versions of SRTM data (NASA et al., 2015). The SRTM data was primary based on the data acquired over the areas between 60° North and 58° South latitudes by the Space Shuttle Endeavour during eleven days since February 11, 2000, to obtain elevation radar data on a near-global scale to provide the digital topographic database of the Earth. The SRTM DEM data is available from January 2015 at the USGS web portal (NASA, 2019). The data was evaluated as highly accurate for use in detecting boundaries of the river basins and lakes in mountainous areas (Czubski, 2013; Chymyrov, 2021). The SRTM acquired data on the Tuyen Quang Reservoir on February 11, 2000, and therefore provided the original topographic features of the reservoir's basin before the dam construction in 2002 (Vietnam Government, 2002). The newer DEM data (acquired after 2002) cannot provide the topographic features of the reservoir bottom after water filling, thus is inappropriate for WD determination in this study. The entire Tuyen Quang Reservoir is in the scene coded "SRTM1N22E105V3," The digital number values range from 10 m to 2,240 m, demonstrating that the water surface is negligible in the study area. Because the SRTM DEM pixels less than 6 are water, and those greater than 10 are land (NASA, 2015). For a better analysis, satellite and DEM data were converted into UTM coordinates using the Projections and Transformations toolset in ArcGIS 10.3 Pro software.

2.3. Image processing methods

2.3.1. Water surface area extraction method

Currently, numerous methods have been developed to delineate WA using moderate-resolution satellite imageries, i.e., Landsat and Sentinel-2. Water indices are widely applied to extract or combine water bodies with other

approaches. Two water indices, including the NDWI and the modified NDWI (MNDWI), often demonstrate high performance and are applied to delineating small waterbodies such as urban lakes (Yang & Chen, 2017). The NDWI was first proposed by McFeeters (1996) for delineating WA from Landsat MSS data. The index is based initially on the difference in the absorption and reflection of light between the water and other features in different frequency bands. As reflections from the water of the visible to infrared bands are gradually weakened, the WA on an image can be delineated with the NDWI by the contrast of the green wavelength with the near-infrared (NIR) wavelength. The following equation calculates the NDWI:

$$NDWI = \frac{\rho_{Green} - \rho_{NIR}}{\rho_{Green} + \rho_{NIR}} \quad (1)$$

where ρ_{Green} and ρ_{NIR} are reflectances of the green band and the NIR band, respectively.

Indeed, NDWI can highlight the waterbodies effectively in most cases. However, it was sensitive to built-up land (Xu, 2006) and to the change in liquid water content of vegetation (Gao, 1996), and therefore often resulted in over-estimated water bodies. For this reason, thus, MNDWI was developed to enhance the water features in the area with a complex landcover system by replacing the NIR band used in NDWI with the shortwaves infrared band (SWIR) to overcome the inseparability of built-up areas (Xu, 2006). The SWIR surrounding 1600 nm was the most feasible way to map the WA (Yang & Chen, 2017). Accordingly, the MNDWI was calculated using the formula:

$$MNDWI = \frac{\rho_{Green} - \rho_{SWIR1}}{\rho_{Green} + \rho_{SWIR1}} \quad (2)$$

where ρ_{Green} and ρ_{SWIR1} are reflectances of the green band and the SWIR1 band of Landsat and Sentinel-2 used in this study.

According to Jensen (2004), the MNDWI helps to classify the satellite image into two classes: (1) water area by positive values; (2) non-water area (built-up land, soils, and vegetation) by negative values. However, MNDWI thresholds for delineating water areas may not equal 0 in all cases due to uncertainties in image processing procedures, particularly for Landsat-7 ETM+ and Landsat-5 TM. Figure 2 shows the selection of MNDWI thresholds to delineate the WA from all Landsat and Sentinel-2 images level 2 used in the study, in which the MNDWI threshold lines fit the boundary of the water surface by the visual interpretation. Accordingly, the MNDWI thresholds to delineate the WA from Landsat-8 and Sentinel-2 images are values larger than 0, and from Landsat-5 TM and Landsat-7 ETM+ are values larger than 0.40 (Fig. 2).

As reported by USGS & NASA (2003; 2004), the Landsat-7 ETM+ experienced a failure of its Scan Line Corrector mechanism in May 2003, resulting in a signal loss in these lines (Fig. 7; Landsat 7 before processing). In this study, used Landsat 7 ETM+ images were gap-filled using the technique developed by Scaramuzza et al. (2004), which was integrated as the plugin "*landsat_gapfill.sav*" in the ENVI 5.4. Indeed, the technique is a linear image transform based on adjusting the standard deviation and mean values of each band of a scene matching another scene acquired near that time, in which the missing lines can be retrieved (Fig. 2; Landsat 7 after processing). This technique was demonstrated as appropriate for monitoring the dynamics of large lakes (e.g., Buma et al., 2018; Ogilvie et al., 2018) and therefore was selected in the study.

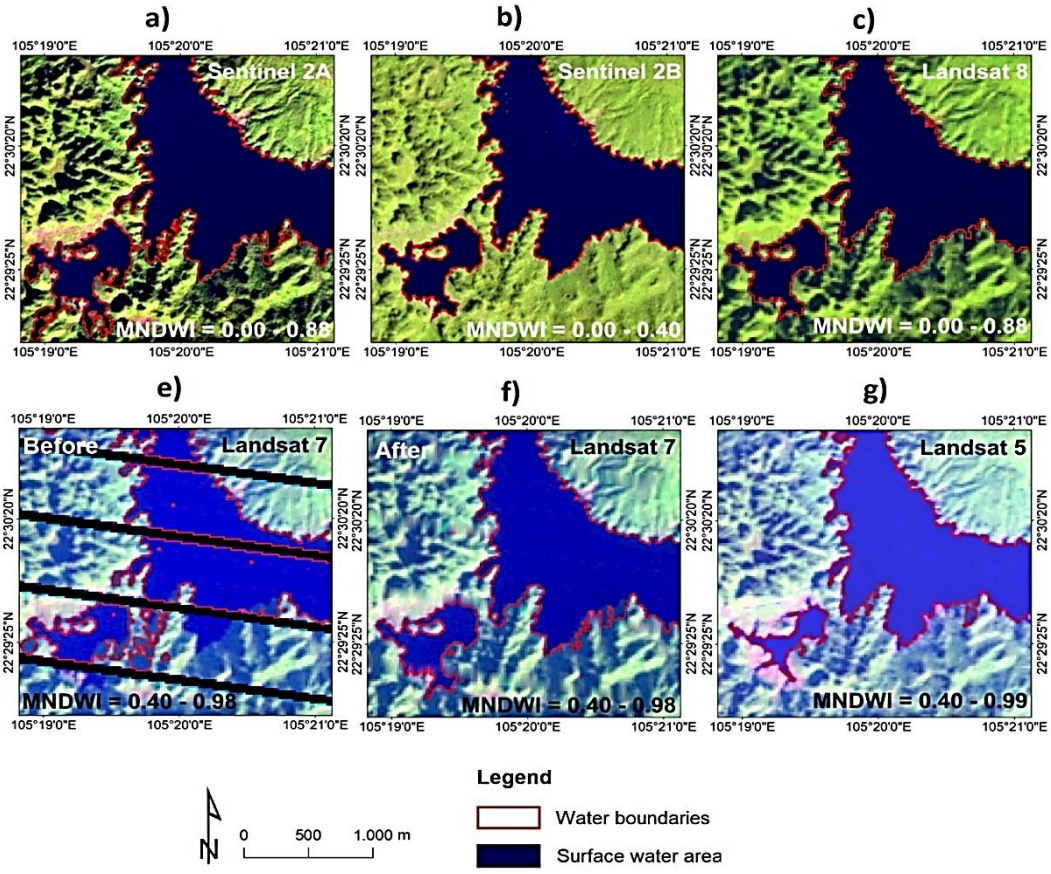

Figure 2. Thresholds for delineating the water surface area from used satellite images. The extent of selected MNDWI threshold on Landsat 7 data before and after gap-filling (e, f)

2.3.2. Water depth and water volume calculations

Water depth (WD) was obtained by calculating the difference in elevations between the pixel of the reservoir shoreline and the pixel:

$$D_i(x,y) = E_s - E_i(x,y) \quad (3)$$

where $D_i(x,y)$ is the WD at pixel i with coordinates (x,y) (m), E_s is the elevation at the current shoreline of the reservoir (m), $E_i(x,y)$ is the elevation at pixel i with coordinates (x,y) (m) as shown in Fig. 3. In which, E_s was defined by overlaying the WA on the DEM image and determined by the elevation value that presents with the highest frequency in pixels matched with the WA borderline. Although, in theory, the pixels matched with the WA borderline is an identical elevation value, if the shoreline features steep cliff topography, its elevation might exceed the factual waterline elevation. Therefore, it is necessary to select E_s following the actual topographical conditions of the reservoir.

Then, the water storage volume (SW) of the reservoir can be calculated using the equation:

$$V = \sum_{i=0}^{n} 900 \times D_i(x,y) \quad (4)$$

where V is the SW of the reservoir at the specified time (m^3), $D_i(x,y)$ is the WD at pixel i with coordinates (x,y) (m), 900 is the area of the pixel i (30 m × 30 m).

Variations of the calculated WD in space can be modeled in the bathymetric map, which was conducted using the density slicing interpolation of the resultant $D_i(x,y)$s over the reservoir. In this study, a bathymetric map was conducted for the data obtained on December 04, 2021, to demonstrate the performance of the methods.

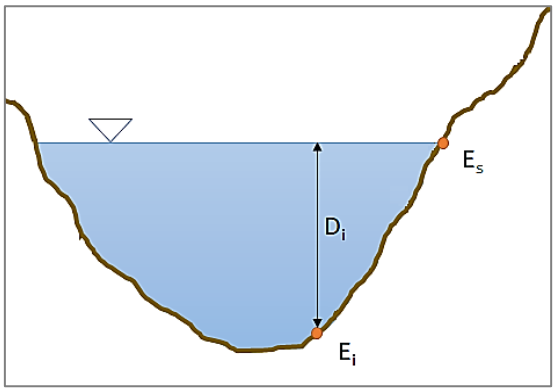

Figure 3. Model the reservoir's cross-section and parameters to calculate water depth from the DEM data. E_s is the elevation at the current shoreline of the reservoir (m), E_i is the elevation at pixel i (m), $D_i(x,y)$ is the WD at pixel i (m).

2.3.3. Accuracy assessment

This study used the Kappa coefficient (K) to assess the accuracy of the WA extraction method because it was recognized as a powerful method for analyzing a single error matrix and for comparing the difference between various error matrices (Smits et al., 1999). When K ≥ 0.90, the MNDWI thresholds were selected for automatic WA extraction from the images. The water level of the Tuyen Quang Reservoir, published on the EVN website (https://www.evn.com.vn), was also used to validate the estimated WA because this parameter is highly correlated to the WA.

Additionally, the Pearson correlation coefficient, the determination coefficient (R^2), and the root mean square error (RMSE) were used to demonstrate the relationship between obtained data and observed factors (rainfall, water level) and validated the DEM data using the topographic map at a scale of 1:50.000 (code: N50NF4843B). The process of monitoring the reservoir's WA and SW from multiple satellite images in this study is presented in Fig. 4.

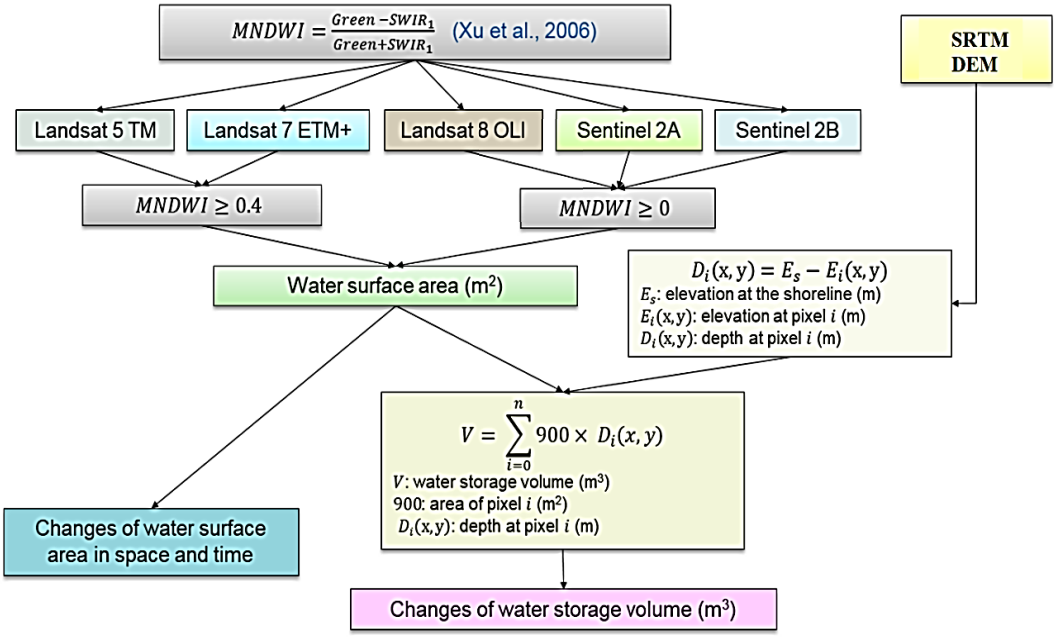

Figure 4. Schematic diagram of the data and methods used in this study

3. Results

3.1. Changes in the water surface area of Tuyen Quang Reservoir

To understand the seasonal variations of WA of Tuyen Quang Reservoir, seven Sentinel-2 images acquired in March, August, November of 2020, and January, June, September, and December of 2021 were used. The resultant maps of WA show that seasonal changes in the reservoir's WA were insignificant; from 6,235 ha in March, dropped to 5,324 ha in August, then increased to 7,066 ha in November of 2020 (Fig. 5). Similarly, in 2021, WA in two months of the wet season (June and September) were 3,828 ha and 5,252 ha, lower than those in December (6,676 ha) and January (6,659 ha). Contrary to expectations, WA was higher in the dry season, when the water discharges decreased due to lack of rainfall. This fact partly reflects the water regulation of the Tuyen Quang Hydropower Plant, i.e., releasing water to generate electricity in the wet season when the available water is higher than the demand, and keeping water in the dry season when the available water is lacking. This result also demonstrates that the reservoir accumulates water at the highest volume at the beginning of the dry season, particularly around November to December.

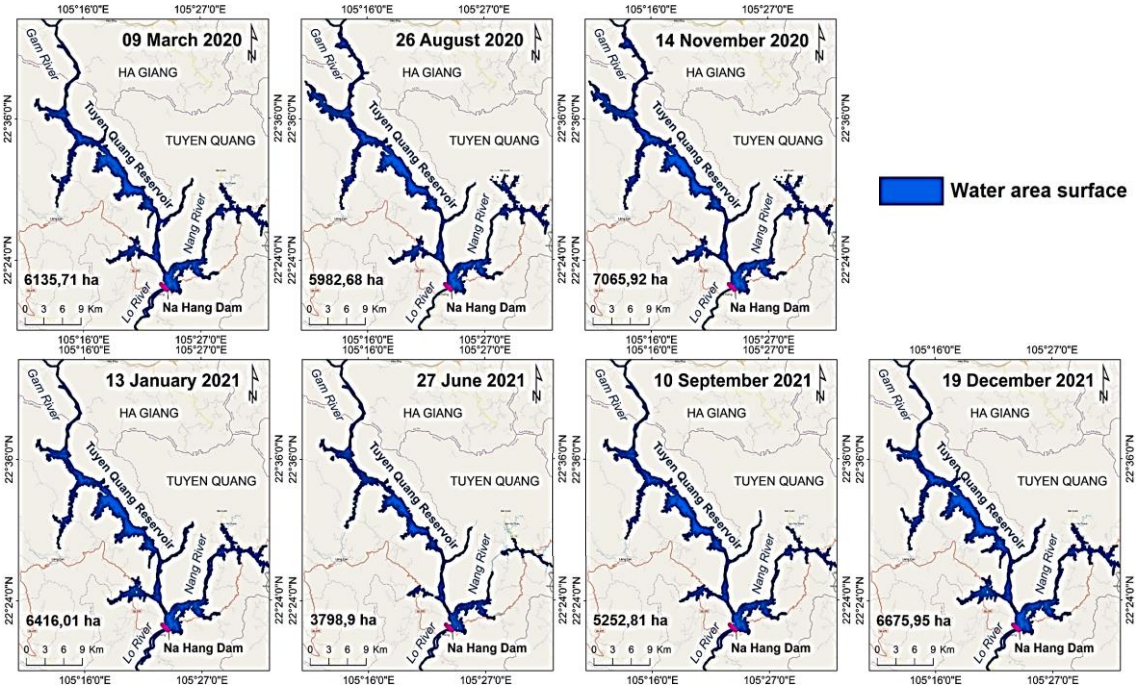

Figure 5. Seasonal variations of water surface area (WA) in March 2020 - December 2021

Fourteen maps recording the WA dynamics in the early dry seasons from 2003 to 2021 are generated and presented in Fig. 6. Accordingly, WA increased rapidly during the construction of the reservoir, i.e., from 2003 to 2007, then fluctuated and gradually increased, reaching to approximately 7,000 ha in 2021. The maps also show that the Na Hang Dam was under construction from 2003–2005 (the dam started construction on December 22, 2002). For this reason, the Tuyen Quang Reservoir was not formed then and was just a section of the Gam River. Since 2006, most of the reservoir's area began to

form, and the reservoir's water level gradually increased, reaching its highest level in 2008, when the Tuyen Quang Hydropower Plant was officially operated. Since then, the WA has not changed significantly, mainly depending on the rainfall over the catchment.

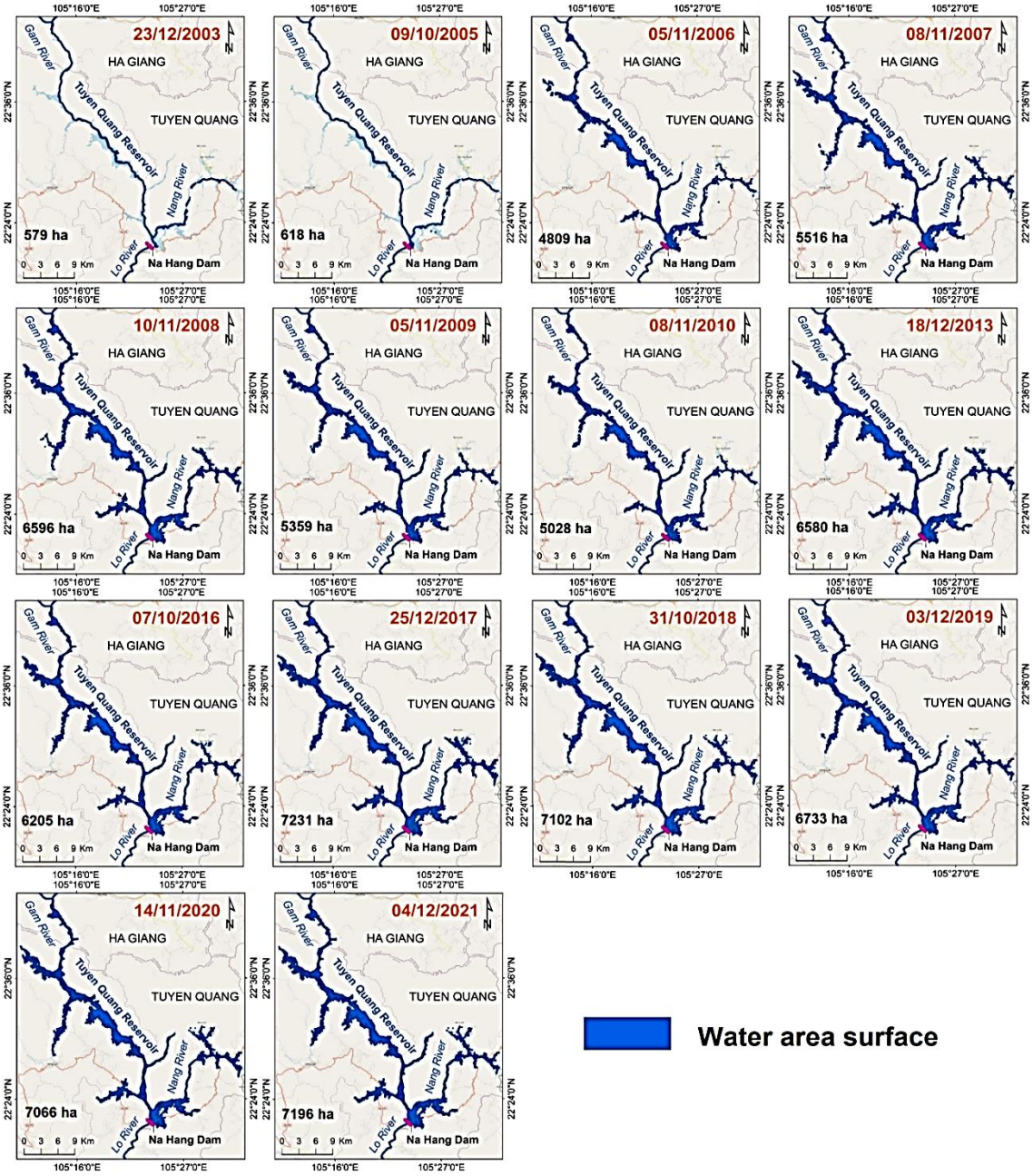

Figure 6. Time-series maps of the water surface area of Na Hang Reservoir detected from Landsat and Sentinel-2 images taken from 2003 to 2021

Figure 7a shows the change map of the WA of the Tuyen Quang Reservoir. According to the map, WA changed mainly in areas with large local streams flowing into the reservoir, such as

Phuc Yen, Lang Can, Thuong Lam, Khau Tinh, and Yen Hoa communes. The highest WA was recorded on November 10, 2008, covering all the large local streams. This result is consistent with the historic severe flood on October 30, 2008, over the northern mountainous region of Vietnam (Chen et al., 2012; Luo et al., 2018). The variations of WA since the Tuyen Quang Hydropower Plant started operation in 2008 are presented in Fig. 7b. Accordingly, the WA was low in 2009 and 2010, corresponding to the drought period in the North of Vietnam (Stojanovic et al., 2020). The WA was highly correlated to the average annual rainfall recorded in Tuyen Quang hydrological meteorology station (r = 0.68), indicating the significant role of rainfall for expanding WA. The estimates of WA for the years 2004, 2011, 2012, 2014, and 2015 were not conducted and presented in Fig. 7 because all Landsat images acquired in the dry season of these years have a high cloud coverage.

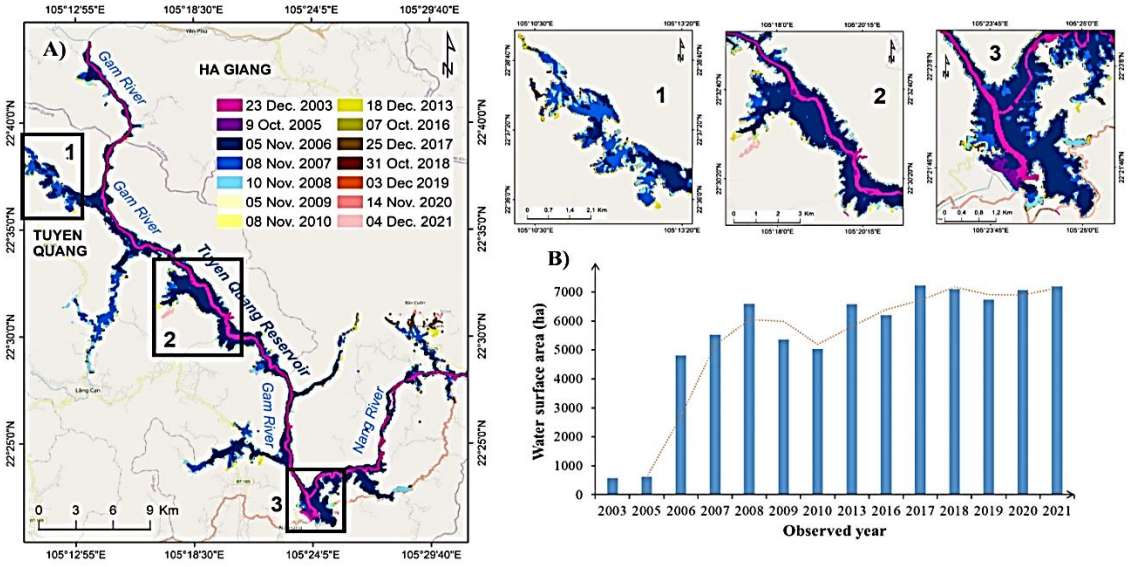

Figure 7. WA's change map (A) and variations during 2003-2021 (B)

3.2. Water depth of Tuyen Quang Reservoir

Accurate water depth (WD) mapping and estimation are of fundamental significance for monitoring the Tuyen Quang Reservoir's SW. As mentioned in the estimation method (*section 2.3.2*), the accuracy of estimated WD is based on the performance of estimated WA and DEM data. This study used the water level at eight-time points in 2021 and 2022 (only eight cloud-free images available for this period), corresponding to seven satellite images acquiring times in Fig. 5 and the image taken on December 4, 2021 (Fig. 6), to validate these estimated WA. The validation result is shown in Fig. 8a by a very tight correlation between published/*in situ* water level and estimated WA (r = 0.96), indicating a high accuracy of the WA estimation. Furthermore, to accurately estimate WD at each pixel within the reservoir, the SRTM DEM data and the water surface boundary must be evaluated with high performance. The reservoir's shoreline can be clearly identified through visual interpretation and MNDWI thresholds. In that case, the SRTM DEM data can also be evaluated using the topographic map established nearly simultaneously. Because the SRTM DEM data of the study area was acquired in 2000; therefore, the data used for a validation was

also extracted from topographic map established in 1999. Accordingly, a hundred spot elevations distributed randomly over the study area and extracted from the Na Hang topographic map at the scale of 1:50,000 (code: code: N50NF4843B) were selected and overlaid with the DEM data (Fig. 8b). A cross-comparison of them with the DEM-derived elevations of their corresponding pixels was conducted and shown in Fig. 8c. The results show that the SRTM DEM data is consistent to the elevations of the study area (R^2 = 0.89; RMSE = 65.8 m, corresponding to 14%) and appropriate for determining the reservoir's WD by Eq. (3).

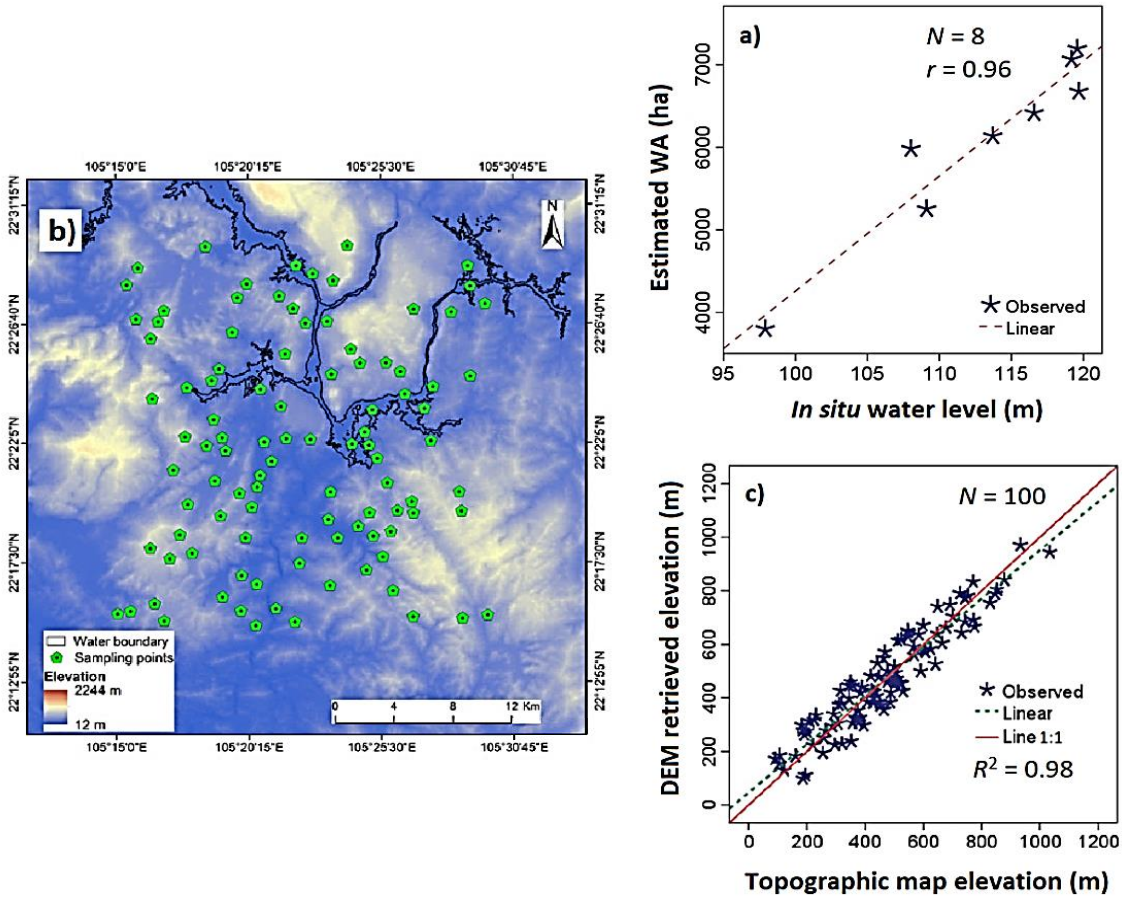

Figure 8. Performance of estimated water surface area (WA) and SRTM DEM data for water depth (WD) estimation: a) The strong correlation of estimated WA and *in situ,* water level demonstrates high accuracy of estimated WA; b) Distribution of a hundred spot elevations extracted from the topographic map (code: N50NF4843B) at the scale of 1:50,000 overlaid the DEM data; and c) The result of the matched-up validation between spot elevations with DEM-derived elevations. *N* is the number of data used for validation

The bathymetric map based on the estimated WD of Tuyen Quang Reservoir on December 04, 2021, is presented in Fig. 9. Accordingly, the mean value of WD of Na Hang Reservoir is 30-40 m, showing an increasing trend from Northwest to Southeast. The highest WD is approximately 112 m, located in the Gam riverbed of the sections

near Lam Binh fishing village and Pac Ta Temple. The statistical results show that the areas with WD of 0-15 m occupy 22% of the reservoir's total area; WD of 15-30 m cover 50% of the reservoir's total area; and WD of 30-45 m account for 22% of the reservoir's total area. The estimated WD also indicates that the upstream water level of Tuyen Quang Reservoir on December 04, 2021, is 112 m, where the upstream water level is defined by the elevation of the reservoir's water surface compared to the mean sea level at Hon Dau Hon Dau Hydro-meteorological station. This result is consistent with the descriptions of Tuyen Quang Reservoir in the Vietnamese Minister's Decision to promulgate the Inter-reservoir Operation Procedures for the Red River basin (2019), in which the reservoir's depth is 112 m.

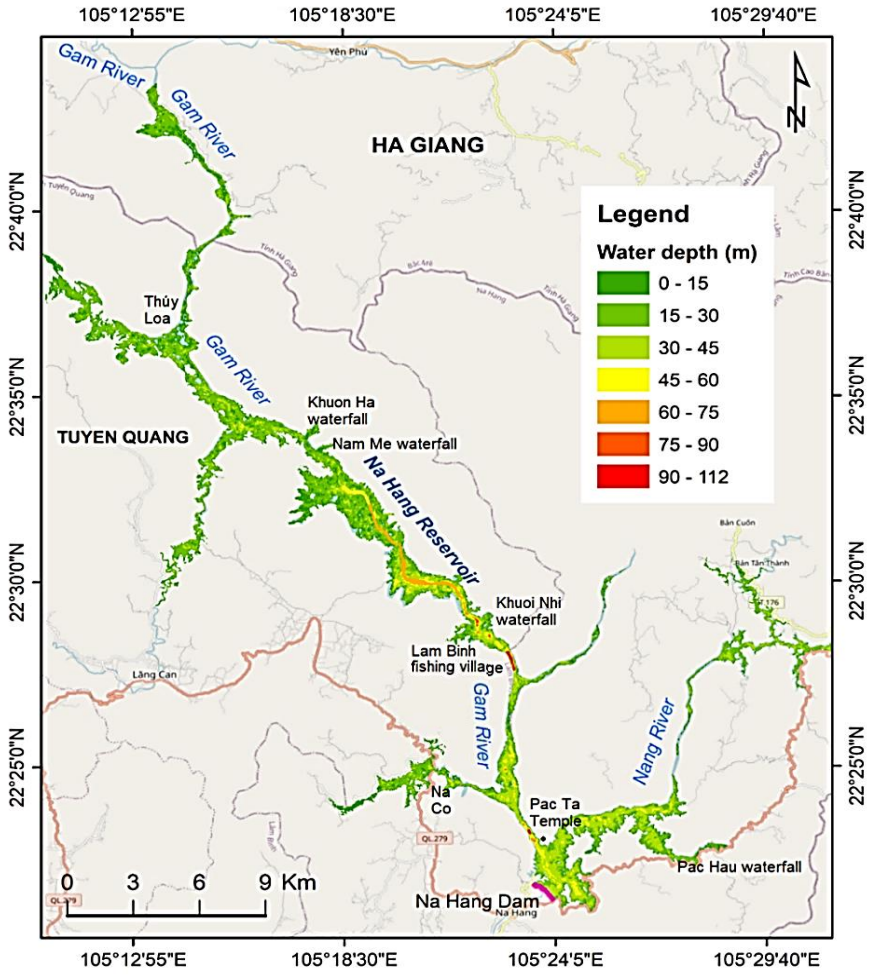

Figure 9. Bathymetric map of Na Hang Reservoir estimated based on the image acquired on December 04, 2021

3.3. Changes in the water surface area of Tuyen Quang Reservoir during 2003-2021

Since WD was accurately estimated using Eq. (3) and the DEM data, Eq. (4) was then applied to calculate the SW of Tuyen Quang Reservoir. Accordingly, the reservoir's SW changes were determined and illustrated in Fig. 10. SW changed negligibly in 2003-2005

(11.8 to 12.6 million m^3), then rose dramatically from 12.6 to 1,346 million m^3 in 2008. After that, SW fluctuated harmoniously with the rainfall and reached 1,684 million m^3 in 2021. From the operation until now, the reservoir's SW has not changed significantly, ranging from 1,500 to 1,600 million m^3, except for two drought years, 2009 and 2010. Compared with the estimated SW published by the Tuyen Quang Hydropower Plant (1,500 to 2,000 million m^3), our results show that the reservoir has accumulated water at the low end of the published values. To reach the value of 2,000 million m^3, more water must be accumulated, particularly in the early dry season, for irrigation and electricity generation.

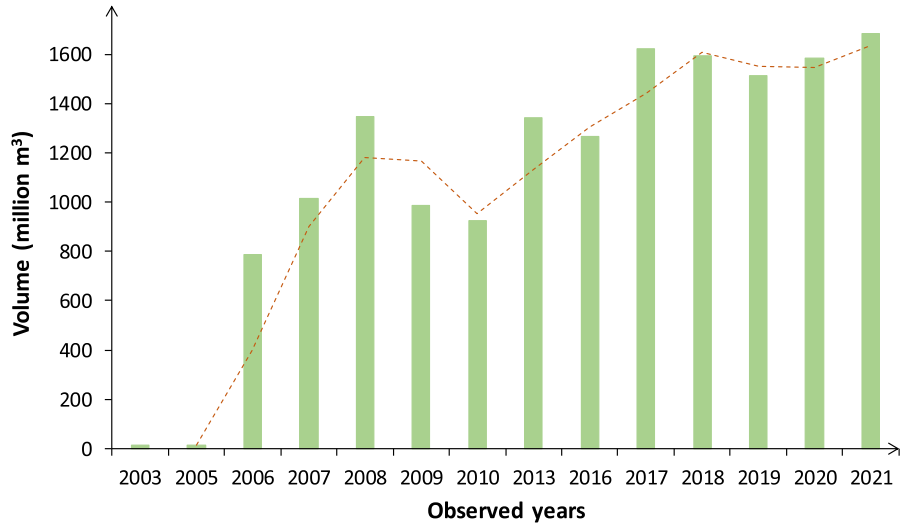

Figure 10. Changes in water storage volume (WA) of Tuyen Quang Reservoir during 2003-2021

4. Discussions

This study demonstrated the capability of remote sensing for monitoring the SW and other specific parameters (e.g., water level, WD, WA) of an impounding reservoir in a mountainous region of Northern Vietnam. In this study, free-of-charge satellite data, such as Landsat series and Sentinel-2 images, and the ASTER DEM, have been exploited successfully in describing the changes in SW, WA and WD of Tuyen Quang Reservoir during 2003-2021. In this study, MNDWI proved excellent for delineating the waterbody of Tuyen Quang Reservoir despite the complex features of the reservoir's catchment terrain. The consistency of estimated WD with the water level published by the Tuyen Quang Hydropower Plant evidenced that the WD estimation method from ASTER GDEM v3 data and the WA extraction is reliable. Our results on monitoring the SW of Tuyen Quang Reservoir during 2003-2021 show that the SW often varies from 1,500 to 1,600 million m^3 and fluctuates depending on the average annual rainfall over the catchment. Seasonally, the SW is high in the dry season and low in the wet season, depending on the water regulation of the Tuyen Quang Hydropower Plant.

Our proposed methodology for monitoring WA, WD, and SW of the Tuyen Quang reservoir in this study can be implemented and applied to other large reservoirs in inaccessible and mountainous regions where the topographic features are not changed rapidly by anthropogenic activities. Indeed, extracting water surface area from multispectral images and calculating WD from DEM data in this study require basic remote sensing skills,

which are entirely consistent with the technical level at the local management. Compared to radar altimetry data, the reasonable estimations of WD at each pixel (30 m × 30 m) in this study help understand the reservoir's bathymetric feature and further provide more accurate estimations of SW than the estimations using altimetry retrieved water level. SWs calculated by altimetry retrieved water level are often over-estimated because the retrieved water level is as flattened as 100% WD for all water pixels within the reservoir (Pham-Duc et al., 2022). Additionally, using radar satellite altimetry for monitoring SW in narrow reservoirs remains challenging due to the data's large antenna footprint and raw space-time resolutions (Tarpanelli & Benveniste, 2019). Therefore, combining DEM and optical satellite data is more convenient and accurate for monitoring SW of narrow and/or small reservoirs.

However, our study is based on satellite data and thus is limited due to the quality of the data itself. Optical satellite data such as Landsat series and Sentinel-2 images used for WA delineation often suffers from limitations due to cloud cover. For this reason, the data is sometimes missing at the specific monitoring time, e.g., in November and December 2014 and 2015. The solution to this problem is to use accessible SAR data, i.e., Sentinel-1 images, which have been demonstrated to be effective for monitoring the seasonal changes of reservoirs (Amitrano et al., 2014; Shen et al., 2022). Furthermore, along with the rapid development of satellite technology, more high-resolution DEM data sources have been released, e.g., TanDEM-X (12 m to 2 m resolution), ALOS PALSAR RTC (12.5 m resolution), making monitoring the SW more convenient and accurate.

The SW is usually calculated using the measured parameters such as the total flow of water in and out and the reservoir's water level following a complex process (TCVN-10778:2015). Therefore, the published data about the water level and flow components do not include SW, WA, and WD. Because the method for determining the water level according to TCVN-10778:2015 is different from the depth estimation in this study, it makes little sense to use the published water level data to evaluate the estimated WD. Also, due to the complexity and uncertainty of the method for determining SW, the Tuyen Quang reservoir's capacity is published only as broad-range estimates, from 1,500 to 2,000 million m^3. That causes a challenge for monitoring changes in SW and validating our estimates.

An additional factor that may affect our estimates is reservoir sedimentation. According to TCVN-10778:2015, reservoir sedimentation can be determined by various methods. However, these methods are based on parameters that cannot be measured directly. Therefore, the reservoir sedimentation of Tuyen Quang Reservoir and other reservoirs can hardly be estimated. Consequently, it is a lack of reservoir sedimentation data to correct estimates. In this case, the published data on the sedimentation velocity of other reservoirs, e.g., Tri An, Nui Coc, and Son La, can be used to understand the possible error of the estimated SW. For Tri An Reservoir, Tan et al. (2014) evidenced the sedimentation velocity of 12 to 132 cm during 1987-2010 (23 years), averaging at 0.6 cm/year using the nuclear technique. The sedimentation velocities in Son La Reservoir and Nui Coc Reservoir were estimated by Hai (2007) and Long (2010) as approximately 1 cm/year and 2 cm/year, respectively, using the HEC-6 model. Based on their results and the operation time of Tuyen Quang Reservoir (14 years, from 2008 to 2022), the error in estimated WD is negligible, ranging from 8.4 to 28 cm, leading to the error of the estimated SW of less than 1 %. In summary, the SRTM DEM data acquired before the dam construction still gives accurate results in monitoring the changes in WD and SW of the reservoir.

It is important to note that the SRTM DEM data used in this study does not accurately reflect the topography of riverbeds, which introduces uncertainty in estimating water depths (WDs) in the original riverbed areas. As a result, the calculated surface water (SW) from pixels in these areas may be underestimated. However, the original riverbed only occupies a small portion of the study area, so the error in estimated SW due to this limitation can be assumed to be insignificant. Moreover, our validation results in Fig. 8c align with previous studies (Wang 2005; Czubski, 2013; Chymyrov, 2021), suggesting the SRTM DEM data is adequate for calculating SW and mapping reservoirs depth for reservoirs constructed after 2000, such as Tuyen Quang Reservoir. Despite the 14 % error in SRTM DEM data, the highest possible error in estimated WD and SW is 28% in two pixels with the highest errors, which is acceptable considering the limited number of such pixels in a normal context. While public data on WD and SW is not available, our results provide valuable insights into the bathymetric features and dynamics of SW in Tuyen Quang Reservoir. Furthermore, our method can also be applied to reservoirs established after February 2000, when the SRTM DEM data was acquired.

5. Conclusions

Our study proposes an easy-to-implement methodology to monitor WA, WD, and SW of impounding reservoirs using multiple free-of-charge satellite data. In the study, the WA can be accurately delineated from the Landsat series and Sentinel-2 images using the MNDWI. In particular, the thresholds of MNDWI for delineating waterbody from Landsat-8 and Sentinel-2 level-2 images are 0-1, and from Landsat-7 ETM+ and Landsat-5 TM level-2 images are 0.4-1. The WD was then calculated using the overlaying analysis of the waterbody boundary over the SRTM DEM v3. data, i.e., the difference between elevation at the reservoir's shoreline and elevation at the calculated pixel. Finally, SW can be retrieved by the sum of all water pixels' volume. The application results for monitoring WA, WD, and SW in Tuyen Quang Reservoir show that the reservoir's WA, WD, and SW change seasonally and annually depending on the rainfall and the water regulation of the Tuyen Quang Hydropower Plant. The WA and SW often range from 6,000 to 7,000 ha and 1,500 to 1,600 million m^3, respectively, except for two dry years, 2009 and 2010. The average WD of Tuyen Quang Reservoir is about 30-40 m. The highest WD was recorded as 112 m in December 2021 on the Gam riverbed at the section near Lam Binh fishing village. The WD and SW estimated in our study agree with published water level data and the Tuyen Quang Reservoir's published description.

Overall, our study has provided valuable insights into the bathymetric features and dynamics of water surface and storage volume in Tuyen Quang Reservoir. Our methodology can be extended to other reservoirs established after February 2000. Future efforts may focus on using other sensor data such as ASTER, Sentinel-1, Sentinel-3, and ALOS PALSAR to fulfill the understanding of reservoir dynamics. Furthermore, to point out their features, our proposed methods can be further applied to other reservoirs in mountainous regions, where the change in topography during the last two decades is negligible. Free altimetry data will be explored in the future as essential auxiliary data to validate the bathymetric estimations.

Acknowledgments

This research is funded by the bilateral collaboration project between Vietnam and Taiwan, grant number NĐT/TW/21/16. The authors thank USGS/NASA and ESA for providing the satellite data.

References

Abrams M., Crippen R., 2019. ASTER GDEM V3 (ASTER global DEM), User Guide Version 1, Japan's Ministry of Economy, Trade and Industry (METI). National Aeronautics and Space Administration (NASA), Jet Propulsion Laboratory/California Institute of Technology, (Technical report), 10p.

Alsdorf D.E., Rodríguez E., Lettenmaier D.P., 2007. Measuring surface water from space. Reviews of Geophysics, 45(2), 2006RG000197.

Amitrano D., Martino G.D., Iodice A., Mitidieri F., Papa M.N., Riccio D., Ruello G., 2014. Sentinel-1 for monitoring reservoirs: A performance analysis. Remote Sensing, 6(11), 10676-10693.

Arsen A., Crétaux J.F., Berge-Nguyen M., Abarca del Rio R., 2013. Remote sensing-derived bathymetry of Lake Poopó. Remote Sensing, 6(1), 407-420.

Avisse N., Tilmant A., Müller M.F., Zhang H., 2017. Monitoring small reservoirs' storage with satellite remote sensing in inaccessible areas. Hydrology and Earth System Sciences, 21(12), 6445-6459.

Biancamaria S., Lettenmaier D.P., Pavelsky T.M., 2016. The SWOT mission and its capabilities for land hydrology. In: Cazenave A., Champollion N., Benveniste J., Chen J. (Eds.), Remote Sensing and Water Resources, Space Sciences Series of ISSI. Springer, Cham., 55, 117-147.

Binh P.D., Son T.S., 2022. Monitoring spatial-temporal dynamics of small lakes based on SAR Sentinel-1 observations: a case study over Nui Coc Lake (Vietnam). Vietnam Journal of Earth Sciences, 44(1), 1-17.

Birkett C.M., 2000. Synergistic remote sensing of Lake Chad: Variability of basin inundation. Remote sensing of environment, 72(2), 218-236.

Bon T.N., Tuyen P.Q., Tung N.D., 2014. Diversity of rare plants in Na Hang Nature Reserve, Tuyen Quang province. Journal of Forestry Science, 4, 3524-3533.

Brooks R.T., Hayashi M., 2002. Depth-area-volume and hydroperiod relationships of ephemeral (vernal) forest pools in southern New England. Wetlands, 22(2), 247-255.

Buma W.G., Lee S.I., Seo J.Y., 2018. Recent surface water extent of Lake Chad from multispectral sensors and GRACE. Sensors, 18(7), 2082.

Chen T.C., Yen M.C., Tsay J.D., Tan Thanh N.T., Alpert J., 2012. Synoptic development of the Hanoi heavy rainfall event of 30-31 October 2008: Multiple-scale processes. Monthly Weather Review, 140(4), 1219-1240.

Chipman J.W., Lillesand T.M., 2007. Satellite-based assessment of the dynamics of new lakes in southern Egypt. International Journal of Remote Sensing, 28(19), 4365-4379.

Chipman J.W., Olmanson L.G., Gitelson A.A., 2009. Remote sensing methods for lake management: A guide for resource managers and decision-makers. North American Lake Management Society. Madison, WI, USA, 126p.

Chymyrov A., 2021. Comparison of different DEMs for hydrological studies in the mountainous areas. The Egyptian Journal of Remote Sensing and Space Science, 24(3), 587-594.

Cohen J., 1960. A coefficient of agreement for nominal scales. Educational and psychological measurement, 20(1), 37-46.

Crétaux J.F., Birkett C., 2006. Lake studies from satellite radar altimetry. Comptes Rendus Geoscience, 338(14-15), 1098-1112.

Crétaux J.F., et al., 2011. SOLS: A lake database to monitor in the Near Real Time water level and storage variations from remote sensing data. Advances in space research, 47(9), 1497-1507.

Crétaux J.F., Abarca-del-Río R., Berge-Nguyen M., Arsen A., Drolon V., Clos G., Maisongrande P., 2016. Lake volume monitoring from space. Surveys in Geophysics, 37(2), 269-305.

Czubski K., 2013. Accuracy of SRTM-X and ASTER elevation data and its influence on topographical and hydrological modeling: case study of the Pieniny Mts. in Poland. International Journal of Geoinformatics, 9(2), 7-14.

Dine M., 2012. Species Conservation Action Plan: Local-based conservation of Tonkin Snub-nosed Monkey at the Na Hang Nature Reserve. People Resources and Conservation Foundation, Hanoi, Vietnam, 36p.

Directorate of Water Resources, (July 18, 2022). Solutions to improve the safety management of dams and irrigation works. Available online: https://www.tongcucthuyloi.gov.vn/tin-hoat-dong-

cua-tong-cuc/nhieu-giai-phap-nang-cao-cong-tac-quan-6368#:~:text=C%E1%BA%A3%20n%C6%B0%E1%BB%9Bc%20hi%E1%BB%87n%20c%C3%B3%2087,ch%E1%BB%A9a%20l%C3%A0%20r%E1%BA%A5t%20quan%20tr%E1%BB%8Dng.

Dost R.J.J., Mannaerts C.M.M., 2008. Generation of lake bathymetry using sonar, satellite imagery and GIS. In Proceedings of the 2008 ESRI international user conference: GIS, Geography in action. San Diego, Florida, USA, 4-8 August 2008, 1-5.

Duan Z., Chu S., Cheng L., Ji C., Li M., Shen W., 2022. Satellite-derived bathymetry using Landsat-8 and Sentinel-2A images: assessment of atmospheric correction algorithms and depth derivation models in shallow waters. Optics Express, 30(3), 3238-3261.

EVN. (access on: 01/12/2022). Summary information on operation of reservoirs. Available online: https://www.evn.com.vn/c3/thong-tin-ho-thuy-dien/Muc-nuoc-cac-ho-thuy-dien-117-123.aspx.

Feyisa G.L., Meilby H., Fensholt R., Proud S.R., 2014. Automated Water Extraction Index: A new technique for surface water mapping using Landsat imagery. Remote Sensing of Environment, 140, 23-35.

Gamble D., Grody E., Undercoffer J., Mack J.J., Micacchion M., 2007. An Ecological and Functional Assessment of Urban Wetlands in Central Ohio. Volume 2: Morphometric Surveys, Depth-Area-Volume Relationships and Flood Storage Function of Urban Wetlands in Central Ohio. Ohio EPA Technical Report WET/2007-3B, Ohio Environmental Protection Agency, Columbus, OH.

Gao B.C., 1996. NDWI A normalized difference water index for remote sensing of vegetation liquid water from space. Remote sensing of environment, 58(3), 257-266.

Gao H., Birkett C., Lettenmaier D.P., 2012. Global monitoring of large reservoir storage from satellite remote sensing. Water Resources Research, 48(9), W09504.

Gleason R.A., Tangen B.A., Laubhan M.K., Kermes K.E., Euliss Jr N.H., 2007. Estimating water storage capacity of existing and potentially restorable wetland depressions in a subbasin of the Red River of the North. U.S. Geological Survey Open-File Report 2007-1159, U.S. Geological Survey, Reston, VA, USA, 89, 36p.

Hai V.H., 2007. Application of HEC-6 model to determine the rising water level and sedimentation for immigration and resettlement. Journal of Science and Technology in Civil Engineering, 1(1), 26-34. https://stce.huce.edu.vn/index.php/vn/article/view/1024.

Hayashi M., Van der Kamp G., 2000. Simple equations to represent the volume area depth relations of shallow wetlands in small topographic depressions. Journal of Hydrology, 237(1-2), 74-85.

Hereher M.E., 2015. Environmental monitoring and change assessment of Toshka lakes in southern Egypt using remote sensing. Environmental Earth Sciences, 73(7), 3623-3632.

Hiep N.Q., Hung N.A., 2019. A method for constructing reservoir area-storage-elevation curve using Sentinel-1 radar remote sensing image. Vietnam Journal of Hydro Meteorology, 706, 10-19. Doi: 10.36335/VNJHM.2019(706).10-19.

Jensen J.R., 2004. Introductory digital image processing: a remote sensing perspective (No. Ed. 3). Prentice-Hall Inc., 621p.

Kellner E., 2021. The controversial debate on the role of water reservoirs in reducing water scarcity. Wiley Interdisciplinary Reviews: Water, 8(3), e1514.

Li J., Roy D.P., 2017. A global analysis of Sentinel-2A, Sentinel-2B and Landsat-8 data revisit intervals and implications for terrestrial monitoring. Remote Sensing, 9(9), 902.

Long L.N., 2010. Assessing the sedimentation of Nui Coc Reservoir and proposing solutions for the reservoir's protection and sustainable use. Journal of Water Resources and Environmental Engineering, 31, 46-51. https://vjol.info.vn/index.php/DHTL/article/view/23015.

Lu S., Ouyang N., Wu B., Wei Y., Tesemma Z., 2013. Lake water volume calculation with time series remote-sensing images. International Journal of Remote Sensing, 34(22), 7962-7973.

Luo P., et al., 2018. Flood inundation assessment for the Hanoi Central Area, Vietnam under historical and extreme rainfall conditions. Scientific reports, 8(1), 1-11.

McFeeters S.K., 1996. The use of the Normalized Difference Water Index (NDWI) in the delineation of open water features. International Journal of Remote Sensing, 17(7), 1425-1432.

Melack J.M., Hess L.L., Sippel S., 1994. Remote sensing of lakes and floodplains in the Amazon Basin. Remote Sensing Reviews, 10(1-3), 127-142.

Morriss B.F., et al., 2013. A ten-year record of supraglacial lake evolution and rapid drainage in West Greenland using an automated processing algorithm for multispectral imagery. The Cryosphere, 7(6), 1869-1877.

NASA, 2015. The Shuttle Radar Topography Mission (SRTM) Collection User Guide V3. United States National Aeronautics and Space Administration (NASA). Online at: https://lpdaac.usgs.gov/documents/179/SRTM_User_Guide_V3.pdf?_ga=2.166866430.1987429350.1676511164-235731952.1654760608.

NASA, 2019. Shuttle Radar Topography Mission (SRTM) Global 1 arc second (GL1). United States National Aeronautics and Space Administration (NASA). Online at: https://www.usgs.gov/centers/eros/science/usgs-eros-archive-digital-elevation-shuttle-radar-topography-mission -srtm-1.

Ogilvie A., Belaud G., Massuel S., Mulligan M., Le Goulven P., Calvez R., 2018. Surface water monitoring in small water bodies: Potential and limits of multi-sensor Landsat time series. Hydrology and Earth System Sciences, 22(8), 4349-4380.

Pardo-Pascual J.E., Almonacid-Caballer J., Ruiz L.A., Palomar-Vázquez J., 2012. Automatic extraction of shorelines from Landsat TM and ETM+ multi-temporal images with subpixel precision. Remote Sensing of Environment, 123, 1-11.

Pope A., Scambos T.A., Moussavi M., Tedesco M., Willis M., Shean D., Grigsby S., 2016. Estimating supraglacial lake depth in West Greenland using Landsat 8 and comparison with other multispectral methods. The Cryosphere, 10(1), 15-27.

Pham-Duc B., Papa F., Prigent C., Aires F., Biancamaria S., Frappart F., 2019. Variations of surface and subsurface water storage in the Lower Mekong Basin (Vietnam and Cambodia) from multisatellite observations. Water, 11(1), 75.

Pham-Duc B., et al., 2022. Monitoring Lake Volume Variation from Space Using Satellite Observations - A Case Study in Thac Mo Reservoir (Vietnam). Remote Sensing, 14(16), 4023.

Scaramuzza P., Micijevic E., Chander G., 2004. SLC gap-filled products phase one methodology. Landsat Technical Notes, 5p.

Shen G., Fu W., Guo H., Liao J., 2022. Water Body Mapping Using Long Time Series Sentinel-1 SAR Data in Poyang Lake. Water, 14(12), 1902.

Smits P.C., Dellepiane S.G., Schowengerdt R.A., 1999. Quality assessment of image classification algorithms for land-cover mapping: A review and a proposal for a cost-based approach. International Journal of Remote Sensing, 20(8), 1461-1486.

Solander K.C., Reager J.T., Famiglietti J.S., 2016. How well will the Surface Water and Ocean Topography (SWOT) mission observe global reservoirs?. Water Resources Research, 52(3), 2123-2140.

Stojanovic M., et al., 2020. Trends and extremes of drought episodes in Vietnam sub-regions during 1980-2017 at different timescales. Water, 12(3), 813.

Swenson S., Wahr J., 2009. Monitoring the water balance of Lake Victoria, East Africa, from space. Journal of Hydrology, 370(1-4), 163-176.

Tan M.T., Van Thuan D., Van Ha V., Tan N.T., Ha T.T.T., Van Tao N., Quan N.C., 2014. Assessment of sedimentation in Tri An reservoir by nuclear technique, geological analyses and GIS. Vietnam Journal of Earth Sciences, 36(1), 51-60.

Tarpanelli A., Benveniste J., 2019. On the potential of altimetry and optical sensors for monitoring and forecasting river discharge and extreme flood events. In Extreme Hydroclimatic Events and Multivariate Hazards in a Changing Environment. Elsevier, 267-287.

The Vietnamese Minister, June 17, 2019. Decision on promulgating the Inter-reservoir Operation Procedures for the Red River basin. No 740/QQD-Ttg. Hanoi 2019. https://www.evn.com.vn/userfile/User/xuantien/files/2019/6/Quyetdinh740TTgCP2019.pdf.

The Vietnamese Minister, June 17, 2019. Decision on promulgating the Inter-reservoir Operation Procedures for the Red River basin.

No 740/QQD-Ttg. Hanoi 2019. https://www.evn.com.vn/userfile/User/xuantien/files/2019/6/Quyetdinh740TTgCP2019.pdf.

Tung H.T., Son N.H., Kim N.Q., Bang N.L., 2020. Monitoring water level and reservoir storage volume from satellite images. Journal of Water resources and Environmental Engineering, 71, 116-123.

Tuyen Quang Provincial People Committee, 2014. Geography of Tuyen Quang Province. Online at: https://tuyenquang.dcs.vn/THITRUCTUYEN/data/202182311649.pdf.

USGS & NASA, 2003. Preliminary assessment of the value of Landsat 7 ETM+ data following Scan Line Corrector Malfunction. Online at: https://www.usgs.gov/media/files/preliminary-assessment-value-landsat-7-etm-slc-data.

USGS & NASA, 2004. SLC-off Gap-Filled Products Gap-fill Algorithm Methodology: Phase 2 Gap-fill Algorithm. Online at: https://www.usgs.gov/media/files/landsat-7-slc-gap-filled-products-phase-two-methodology.

Vanthof V., Kelly R., 2019. Water storage estimation in ungauged small reservoirs with the TanDEM-X DEM and multi-source satellite observations. Remote Sensing of Environment, 235, 111437.

Verpoorter C., Kutser T., Seekell D.A., Tranvik L.J., 2014. A global inventory of lakes based on high-resolution satellite imagery. Geophysical Research Letters, 41(18), 6396-6402.

Vietnam Government, 2002. Prime Minister's Decision on approval of investment for Na Hang hydropower project, No. 288/QĐ-TTg, issued on April 19 2002. Online at: https://thuvienphapluat.vn/van-ban/Dau-tu/Quyet-dinh-so-288-QD-TTg-nam-2002-cua-Thu-tuong-Chinh-phu-phe-duyet-du-an-thuy-dien-Na-Hang-165663.aspx.

Vietnam National Standards, 2015. Reservoirs - Determination of specific water levels. TCVN 10778: 2015. https://vanbanphapluat.co/tcvn-10778-2015-ho-chua-xac-dinh-cac-muc-nuoc-dac-trung.

Wang Y., Liao M., Sun G., Gong J., 2005. Analysis of the water volume, length, total area and inundated area of the Three Gorges Reservoir, China using the SRTM DEM data. International Journal of Remote Sensing, 26(18), 4001-4012.

Wang X., Cheng X., Gong P., Huang H., Li Z., Li X., 2011. Earth science applications of ICESat/GLAS: A review. International Journal of Remote Sensing, 32(23), 8837-8864.

Wang W., Yang X., Yao T., 2012. Evaluation of ASTER GDEM and SRTM and their suitability in hydraulic modelling of a glacial lake outburst flood in southeast Tibet. Hydrological Processes, 26(2), 213-225.

World Commission on Dams, 2000. Dams and development: A new framework for decision-making: The report of the world commission on dams. Earthscan.

Xu H., 2006. Modification of normalised difference water index (NDWI) to enhance open water features in remotely sensed imagery. International Journal of Remote Sensing, 27(14), 3025-3033.

Yang X., Chen L., 2017. Evaluation of automated urban surface water extraction from Sentinel-2A imagery using different water indices. Journal of Applied Remote Sensing, 11(2), 026016.

Yang X., Chen L., 2017. Evaluation of automated urban surface water extraction from Sentinel-2A imagery using different water indices. Journal of Applied Remote Sensing, 11(2), 026016.

Yang X., Chen Y., Wang J., 2020. Combined use of Sentinel-2 and Landsat 8 to monitor water surface area dynamics using Google Earth Engine. Remote Sensing Letters, 11(7), 687-696.

Yoshikawa S., Cho J., Yamada H.G., Hanasaki N., Khajuria A., Kanae S., 2013. An assessment of global net irrigation water requirements from various water supply sources to sustain irrigation: rivers and reservoirs (1960-2000 and 2050). Hydrol. Earth Syst. Sci. Discuss, 10(1), 1251-1288.

Zarfl C., Lumsdon A.E., Berlekamp J., Tydecks L., Tockner K., 2015. A global boom in hydropower dam construction. Aquatic Sciences, 77(1), 161-170.

Zhang G., Xie H., Kang S., Yi D., Ackley S.F., 2011. Monitoring lake level changes on the Tibetan Plateau using ICESat altimetry data (2003-2009). Remote Sensing of Environment, 115(7), 1733-1742.